Soft Matter

PAPER

View Article Online
View Journal | View Issue

Cite this: *Soft Matter*, 2015, **11**, 7606

Effects of magnetic field gradients on the aggregation dynamics of colloidal magnetic nanoparticles†

D. Heinrich,[a] A. R. Goñi,*[bc] T. M. Osán,*[d] L. M. C. Cerioni,[e] A. Smessaert,[f] S. H. L. Klapp,[f] J. Faraudo,[c] D. J. Pusiol[g] and C. Thomsen[a]

Received 6th March 2015,
Accepted 2nd August 2015

DOI: 10.1039/c5sm00541h

www.rsc.org/softmatter

We have used low-field ^{1}H nuclear-magnetic resonance (NMR) spectroscopy and molecular dynamics (MD) to investigate the aggregation dynamics of magnetic particles in ionic ferrofluids (IFFs) in the presence of magnetic field gradients. At the beginning of the experiments, the measured NMR spectra were broad and asymmetric, exhibiting two features attributed to different dynamical environments of water protons, depending on the local strength of the field gradients. Hence, the spatial redistribution of the magnetic particles in the ferrofluid caused by the presence of an external magnetic field in a time scale of minutes can be monitored in real time, following the changes in the features of the NMR spectra during a period of about an hour. As previously reported [Heinrich *et al.*, *Phys. Rev. Lett.*, 2011, **106**, 208301], in the homogeneous magnetic field of a NMR spectrometer, the aggregation of the particles of the IFF proceeds in two stages. The first stage corresponds to the gradual aggregation of monomers prior to and during the formation of chain-like structures. The second stage proceeds after the chains have reached a critical average length, favoring lateral association of the strings into hexagonal zipped-chain superstructures or bundles. In this work, we focus on the influence of a strongly inhomogeneous magnetic field on the aforementioned aggregation dynamics. The main observation is that, as the sample is immersed in a certain magnetic field gradient and kept there for a time τ_{inh}, magnetophoresis rapidly converts the ferrofluid into an aggregation state which finds its correspondence to a state on the evolution curve of the pristine sample in a homogeneous field. From the degree of aggregation reached at the time τ_{inh}, the IFF sample just evolves thereafter in the homogeneous field of the NMR spectrometer in exactly the same way as the pristine sample. The final equilibrium state always consists of a colloidal suspension of zipped-chain bundles with the chain axes aligned along the magnetic field direction.

1 Introduction

Magnetic nanoparticles (NPs) play at present a key role in a number of technological contexts such as storage media, design of new functional materials and medical applications, among others. In many cases, particles having permanent magnetic dipole moments are dispersed in a non-magnetic carrier liquid such as water or oil, resulting in a colloidal suspension often referred to as "ferrofluids" (FFs).[1] Typical FFs involve fairly spherical particles with sizes of about a few to several tens of nanometers. Because of their small dimensions, the particles exhibit magnetic single-domain structure and superparamagnetic behavior in the presence of external magnetic fields.[2–5] The resulting long-range dipole–dipole interactions between magnetic particles play an important role in their cooperative behavior. In fact, even at low fields and small packing fractions, the energetic preference of head-to-tail configurations leads to the formation of chains, as experimentally observed.[6–12]

[a] *Institut für Festkörperphysik, EW 5–4, Technische Universität Berlin, Hardenbergstrasse 36, D-10623 Berlin, Germany*
[b] *ICREA, Passeig Lluís Companys 23, E-08010 Barcelona, Spain*
[c] *Institut de Ciència de Materials de Barcelona (ICMAB-CSIC), Campus UAB, E-08193 Bellaterra, Spain. E-mail: goni@icmab.es*
[d] *Facultad de Matemática, Astronomía y Física. Universidad Nacional de Córdoba and Consejo Nacional de Investigaciones Científicas y Técnicas (CONICET)., Av. Medina Allende s/n. Ciudad Universitaria, X5000HUA Córdoba, Argentina. E-mail: tosan@famaf.unc.edu.ar*
[e] *SPINLOCK S.R.L and Consejo Nacional de Investigaciones Científicas y Técnicas (CONICET), Av. Sabattini 5337, Ferreyra, X5016LAE Córdoba, Argentina*
[f] *Institute of Theoretical Physics, Sekr. EW 7–1, Technical University Berlin, Hardenbergstrasse 36, D-10623 Berlin, Germany*
[g] *Consejo Nacional de Investigaciones Científicas y Técnicas (CONICET), Av. Rivadavia 1917, Ciudad Autónoma de Buenos Aires, Argentina*

† Electronic supplementary information (ESI) available. See DOI: 10.1039/c5sm00541h

At larger packing fractions and/or with nanoparticles showing strong magnetic coupling, the application of an external (static) magnetic field can trigger the formation of superstructures consisting of a sort of aligned chain bundles.[11–16] Magnetic-particle suspensions are, thus, of fundamental interest because they constitute prime examples of complex fluids, whose internal structure, phase behavior and dynamic rheological properties can be efficiently controlled by external parameters.[17,18]

Self-assembly phenomena such as chain formation in systems with strong dipole–dipole interactions are a topic of considerable theoretical interest. For example, recent theoretical studies on systems without external fields employ concepts from theories of network formation[19] and the percolation or polymerization transition[20] to explain the zero-field behavior (particularly the absence of conventional vapor–liquid coexistence) observed in computer simulations.[21,22] The structure formation within a (homogeneous) field, including the formation of field-aligned chains, columns and crystals, has been investigated in various studies.[23–26] A related problem is the structure formation in electrorheological (ER) and magnetorheological (MR) fluids (systems of polarizable colloids in electric/magnetic fields), which also display column and crystal formation.[24,25] These phenomena have been explained, at least partially, by ground state calculations.[27,28] A central (and somewhat counterintuitive) point is that under certain conditions, neighboring aligned dipolar chains can attract each other.[6] In fact, magnetic energy calculations clearly show that for long enough chains (more than 14 particles), the formation of thicker aggregates due to lateral aggregation of chains is favored instead of longer chains.[29] To a certain extent, the aggregation phenomena we are dealing with in ferrofluids are closely related to the so-called field-directed self-assembly. Electric and/or magnetic fields can generate orientation-dependent, long range interactions between colloidal particles, which direct their assembly into highly ordered structures, such as small ordered clusters, chains, and large crystalline lattices.[30,31] In the case of ferrofluids, the attractive head-to-tail interaction between the permanent magnetic dipoles that leads to the formation of chain-like structures oriented along an external magnetic field can be switched on and off with the very same field. Hence, directed self-assembly processes might be exploited for the development of new functional materials with specific and/or switchable properties. Current research in the area of diagnostic tests and experimental therapies for malignant masses often requires the utilization of FFs because they can be used to deliver drugs or to absorb toxins inside the body depending on which coating is used for the particles.[32] Due to their capability to reach the site of concern, another area of use of FFs is hyperthermia therapy.[33] In all these cases, solutions containing magnetic particles are injected into a biological system and are guided to the site of interest by means of magnetic fields. The use of inhomogeneous magnetic fields to take away the magnetic particles from a solution is known as magnetic separation or magnetophoresis and has provided new techniques capable of improving standard technologies, especially in biotechnological applications.[34] As a result, the manipulation of magnetic particles by using inhomogeneous magnetic fields is a topic of great interest in a wide range of research and technological areas.[29,35]

The clustering dynamics of magnetic particles in steric[36] and ionic[9,37] ferrofluids was previously investigated by means of Raman and NMR spectroscopy.[38] In Raman scattering experiments, the change in the intensity of the stretching vibrational band of water was used to monitor field-induced variations in local particle concentration. In particular, the time dependence of cluster building and its dissociation in different external inhomogeneous magnetic fields up to 350 mT were studied by these methods. As a result, the time evolution of both aggregation/disaggregation processes showed an exponential behavior with characteristic times of the order of 100 s at room temperature.[9] On the other hand, NMR spectroscopy was also used to study the equilibrium structure as well as the dynamics of aggregation of magnetic nanoparticles. An advantage of NMR with respect to Raman is that the former technique can distinguish between contributions coming from distinct magnetic environments of water protons at different distances from the magnetic nanograins.[38] As nanograins form more complex structures, the strength of the magnetic field gradients sensed by the protons in their restricted diffusion changes, which leads to the concomitant reshaping of the NMR spectrum. This was used to retrieve the appearance and pace of formation of the chain-like structures and superstructures.[9,16]

In a previous work, we have studied the aggregation dynamics of magnetic nanoparticles in an ionic ferrofluid (IFF) in the presence of a spatially homogeneous magnetic field by means of low-field NMR spectroscopy and molecular dynamics (MD) simulations.[16] In that case, the results showed that IFFs exhibit a stepwise association process from ensembles of monomers over string-like chains to bundles of hexagonal zipped-chain patches.[16] Besides, it was shown that attractive van der Waals interactions due to charge-density fluctuations in the magnetic particles were instrumental for the stabilization of the superstructures against thermal dissociation. In contrast, here we consider the effects of an inhomogeneous field on the aforementioned structure-formation dynamics. In principle, the main difference from the point of view of the physical mechanisms leading to aggregation/dissociation processes is the presence of magnetic field gradients, which induce magnetophoresis in the magnetic colloid. That means that there is an effective force acting upon the magnetic dipoles of the nanoparticles, which drives them towards the regions of maximum magnetic strength. This mechanism adds to the ones associated with electrostatic repulsion, the magnetic dipole–dipole attraction and van der Waals interactions between chain segments. As this might have a strong influence on the formation dynamics, we focus our attention on the effects of magnetophoresis, always compared with the case in which the state of the magnetic colloid evolves in a homogeneous field.

2 Framework

2.1 NMR lineshape

The general expression for a quadrature-detected NMR signal can be described as follows:[39]

$$S(t) = C\mathrm{e}^{2\pi(\mathrm{i}\nu_0-\gamma)t}, \quad (1)$$

where ν_0 denotes the Larmor frequency, C represents the (complex) signal amplitude and γ is the inverse of a (real) time constant related to the spin–spin relaxation time of the magnetic dipoles and the homogeneity of the magnetic field distribution around its mean value $\mathbf{B}_0$. In praxis, the Fourier transform (FT) of eqn (1) is used, converting the time-dependent signal called free-induction decay (FID) into a function of frequency.[39,40] The result is a complex NMR spectrum described by the following equation:

$$S(\nu) = C\left(\frac{\gamma^2}{\gamma^2 + (\nu-\nu_0)^2} - \mathrm{i}\frac{\gamma\cdot(\nu-\nu_0)}{\gamma^2 + (\nu-\nu_0)^2}\right). \quad (2)$$

The real and imaginary parts of eqn (2) are called absorption and dispersion Lorentzian, respectively. Usually only the real part of the spectrum is used for the analysis of a NMR experiment. However, due to the fact that the NMR signal can be affected by a phase factor, in practice the parameter C is also complex. By writing $C = Ae^{i\varphi}$, with A being a positive real constant and $\varphi \in [0,2\pi]$ a phase factor, the real part of eqn (2) can be written as:

$$S_R(\nu) = \frac{A\cdot\gamma}{\gamma^2 + (\nu-\nu_0)^2}[\gamma\cos\varphi + (\nu-\nu_0)\sin\varphi], \quad (3)$$

where γ represents the half-linewidth of the Fourier-transformed NMR signal. Note that, the imaginary part of the NMR spectrum is simply obtained by a phase shift of $\pi/2$ of the real part $S_R(\nu)$. For convenience we have expressed $S_R(\nu)$ in terms of the frequency shift $\nu - \nu_0$ in units of Hz, referred to the resonance frequency ν_0 of free protons in pure water.

2.2 Molecular dynamics (MD) simulations

In order to obtain further insight into the association processes, at least on a qualitative level, we launched MD simulations using a simplified model consisting of about thousand spherical particles with diameters σ and magnetic dipole moments $\boldsymbol{\mu}_i$ completely aligned along the field direction. The field is assumed to be homogeneous. The isotropic part of the two-particle interaction at distance $r_{ij} = |\mathbf{r}_i - \mathbf{r}_j|$ can be described by means of a (truncated and shifted) Lennard-Jones (LJ) potential of the form,

$$u_{LJ}(r_{ij}) = 4\varepsilon((\sigma/r_{ij})^{12} - (\sigma/r_{ij})^6), \quad (4)$$

where the van der Waals (vdW) term ($\propto r_{ij}^{-6}$) models the attractive (induced-dipole) interactions due to charge density fluctuations in the nanoparticles. The anisotropic contribution mimicking magnetic dipole–dipole (DD) interactions is well described by a screened, short-ranged potential

$$u_{DD}^{scr}(r_{ij}) = \frac{\mu_0}{4\pi}(\boldsymbol{\mu}_i\nabla_i)\left(\boldsymbol{\mu}_j\nabla_j\right)\left[\exp(-\kappa r_{ij})/r_{ij}\right], \quad (5)$$

with $\kappa\sigma = 1$,[41] where $\mu_0 = 4\pi 10^{-7}$ NA^{-2} is the magnetic permeability of free space. A somewhat strong assumption is that we restrict ourselves to two-dimensions (2D) by considering a slice through the real system. In this way, a computation involving many particles is affordable but the physics is not qualitatively altered. MD simulations were carried out at a 2D packing fraction close to the experimental situation of $\phi_0 = (\pi/4)\rho\sigma^2 = 0.015$, with ρ being the number density. Furthermore, the dimensionless LJ parameter $\varepsilon^* = \varepsilon/k_BT = 1.0$ (with $k_B = 1.3805 \times 10^{-23}$ J K^{-1} and T being the Boltzmann constant and the absolute temperature, respectively), and the dipolar coupling strength $\lambda = \frac{\mu_0 {m_s}^2}{4\pi k_B T\sigma^3} = 7$. Here $m_s = |\boldsymbol{\mu}_i|$ is the saturation magnetization which is a function of the particle size. The value of the dimensionless parameter λ was chosen based on previous simulation studies of 2D dipolar systems,[23] from which pronounced aggregation is known to occur. Finally, calculations were performed at constant temperature using a standard leap-frog algorithm[42] with a time step of $\Delta t = 0.0025$ to solve the (translational) equations of motion. Typical MD runs consisted of about 10^6 time steps for equilibration, followed by a production period of about $2 \times 10^6 \Delta t$.

2.3 Theory of chain formation and morphology of the aggregates

The dipole–dipole interaction energy between two superparamagnetic particles with a field-induced magnetic dipole moment m separated by a distance r can be written as:

$$U_{DD} = \frac{\mu_0}{4\pi}\frac{m^2}{r^3}\left[1 - 3\cos^2\theta\right], \quad (6)$$

where θ is the angle between the direction of the external magnetic field and the line joining the centers of the two particles. The relevance of this attractive particle–particle interaction for the aggregation of the magnetic particles dispersed in the fluid depends much on its strength, as compared with thermal energy. The ratio between both energies can be taken as a magnetic coupling parameter which is defined as:[43,44]

$$\Gamma = \frac{|U_{DD}^{max}|}{k_BT} = \frac{\mu_0 {m_s}^2}{2\pi\sigma^3 k_B T}. \quad (7)$$

By comparing eqn (7) and the definition of the dipolar coupling strength λ given above, it holds $\Gamma = 2\cdot\lambda$. Physically, $\Gamma \gg 1$ is indicative of a scenario dominated by magnetic interactions (favoring aggregation), whereas $\Gamma \ll 1$ corresponds to a situation where thermal agitation is predominant (favoring dissociation). The Γ values for conventional ferrofluids typically span a wide range from 0.5 up to 40.[44] Nevertheless, the possibility of chain formation depends not only on the magnetic coupling Γ but also on the volume fraction ϕ_0 of magnetic particles dispersed in the fluid. It has been demonstrated that the average length of chains, if formed, can be computed from the number N^* of monomers that remains aggregated on average in thermal equilibrium, as:[44,45]

$$N^* = \sqrt{\phi_0 e^{\Gamma-1}}. \quad (8)$$

A value of $N^* \leq 1$ means no-chain formation, whereas for $N^* > 1$ chains are present in the fluid with a length distribution characterized by a probability $p(N) \sim \exp\left(-\frac{N}{N^*}\right)$ of finding chains with N particles.[45]

As far as the morphology of the superstructures or chain bundles is concerned (which are built-up by subsequent collisions of already formed chains), it has been shown by magnetic

energy calculations that there are two possibilities.[29] After collision of two chain pieces of length N and N', either they form a longer single chain of length $N + N'$ (tip-to-tip aggregation), or they form a ticker chain or bundle (lateral aggregation). By summing up all dipole–dipole interactions between pairs of the $N + N'$ particles, it turns out that for the tip-to-tip aggregation, the magnetic interaction energy rapidly levels at a value of $U \approx -3.27U_0$, independent of the chain length, with U_0 given by[29]

$$U_0 = 4k_BT\cdot\Gamma. \quad (9)$$

On the contrary, for lateral aggregation the interaction energy decreases linearly with the chain length with slope $\frac{\Delta U}{\Delta N} \approx -0.35U_0$. As a consequence, for sufficiently long chains ($N > 14$) one would expect from simple energetics arguments that lateral aggregation into zipped-chain bundles becomes more favorable than mere extensions in chain length.[29]

3 Experimental

The sample consisted of an electrostatically stabilized ferrofluid composed of charged magnetite (Fe_3O_4) grains dispersed in water with a particle concentration in volume $\phi_0 = 0.01$. HCl acid was employed to stabilize the sample with a pH = 3. Sample characterization by means of dynamic light scattering (DLS) showed that primary particles of less than 10 nm in size irreversibly agglomerated to form stable grains of about 145 nm in diameter, on average. The colloidal suspension of agglomerates exhibits a polydispersity index of around 0.2, which is typical for this kind of ferrofluid, and is totally stable over periods of many months, provided solvent evaporation or changes in pH are avoided. Magnetization measurements indicated superparamagnetic behavior[2–5] with a resulting value for the magnetic dipole at a saturation of $m_s = 2.744 \times 10^{-17}$ J T^{-1}. Further details of the preparation, characterization and a digression on the colloidal stability of the ionic ferrofluids used in this work can be found in the ESI.†[49] About 14 ml of the fluid was loaded into a small sealed plastic vial and placed in the bore of a low-resolution SpinLock SLK-100 NMR spectrometer equipped with two permanent magnets generating a magnetic field of $B_0 = 225$ mT. Magnetic field homogeneity was measured to yield 22 ppm with a field gradient of 5 μT cm^{-1}.

The NMR experiments ran as follows. First, the NMR spectra of the pristine IFF sample were taken subsequently in the presence of the homogeneous magnetic field B_0 of the NMR spectrometer every 30 s for more than 3000 s. Next, in order to study the influence of a magnetic field gradient on the aggregation dynamics, several sets of NMR spectra were acquired after the IFF sample was subjected to a spatially inhomogeneous field for a certain time. For this purpose, we placed the IFF sample in the vial on top of a permanent magnet, as illustrated in Fig. 1. The vial was kept at this exact position at the edge of the magnet, where its stray field produces an average gradient of about 5 T m^{-1}, for different times τ_{inh} up to 240 s. After this dwelling time, the sample was introduced into the NMR spectrometer as fast as possible (total time ~1 min) for monitoring the structure and superstructure formation dynamics, again measuring a spectrum every 30 s for up to 3000 s. The evolution of the NMR signal from the water protons is thus continuously monitored and from a line-shape analysis using eqn (3) we obtain the amplitude, resonance frequency shift, linewidth and phase as a function of time and for the different dwelling times τ_{inh} in the field gradient of the permanent magnet. After each experimental run, the sample was sonicated for several minutes to return it to its initial state (reversible dissociation of all chain-like aggregates). This was confirmed by the reproducibility of the NMR spectrum which exhibited, within the experimental uncertainty, the same four parameters after sonication as those of the pristine sample at the beginning of a run.

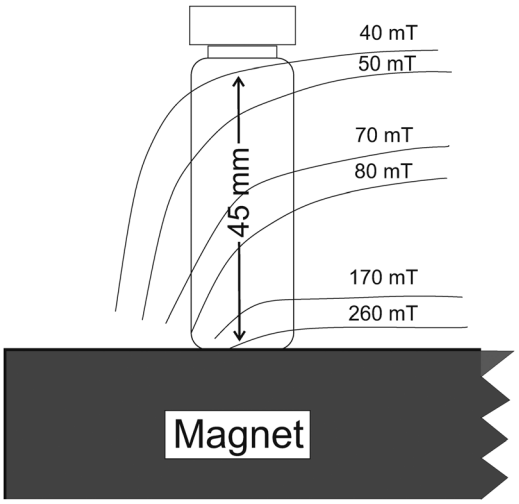

Fig. 1 Sketch of the permanent magnet and the lines (surfaces) of constant magnetic field strength, as indicated, which have been previously mapped out using a Hall probe. The sample was placed always at the same marked position near the edge of the magnet. The resulting gradient of the magnetic field is roughly 5 T m^{-1}.

4 Results and discussion

Fig. 2 shows two representative examples of the NMR spectra (blue open symbols) of the pristine sample, which has not been subjected to any magnetic field gradient before, consisting of the real as well as the imaginary part of the Fourier transform of the free-induction decay (FID) signal, measured at two different times of the same run. The curves in Fig. 2a and b correspond to the measurement performed 30 s after the pristine IFF sample was introduced into the NMR spectrometer, whereas Fig. 2c and d display the results obtained at a much later stage (3000 s), for which equilibrium in the homogeneous field was practically reached. The red solid curves correspond to the NMR lineshape function fitted to the data points. This function is constructed by adding an expression like eqn (3) for the real part of the NMR signal for each of the three resonance lines apparent in the spectrum (black dashed lines). From such

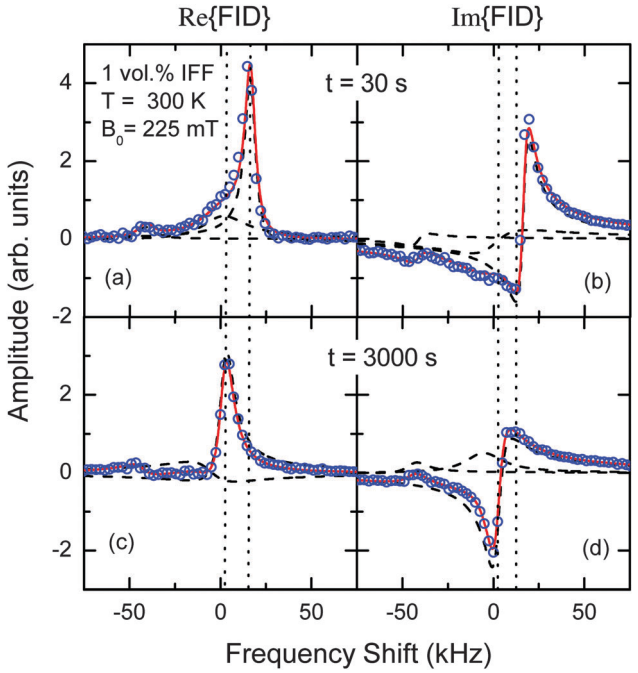

Fig. 2 Real and imaginary parts of the Fourier transformed FID signal (open blue symbols) at two different times for the pristine sample, *i.e.*, without having experienced any field gradient, (a and b) at the beginning of the measurement and (c and d) after 3000 s. The solid red lines correspond to the total fitting function, whereas the dashed black lines represent each of the three resonances composing the full signal.

lineshape fitting we extract the values of the four parameters (A, ν_0, γ, and φ) as a function of time for each resonance peak. The imaginary part is simply obtained by using eqn (3) with a shifted phase ($\pi/2 - \varphi$), keeping the same values for the rest of the parameters.

The main peak in Fig. 2a at the beginning of the experiment exhibits a large frequency shift of about 17 kHz with respect to the pure water signal, thus being associated with water protons within the solvation layer near and around the magnetic poles of the nanograins. The large frequency shift indicates that these protons are sensing a strong average magnetic field, whereas the relatively small linewidth speaks for a largely restricted motion in a region with a fairly narrow field distribution.[16,38] The much broader secondary feature centered at around 0 kHz, in contrast, is assigned to the signal from water molecules moving freely within the interstitial volume between magnetic particles but far away from them. In this case, although protons feel an almost vanishing average field, during the time of 11 ms over which the NMR signal is collected, they diffuse in vast regions with a large distribution of magnetic fields. This is the physical reason for the counter-intuitively large linewidth.[16,38] Finally, the feature peaking at −45 kHz is attributed to the signal produced by the protons of the HCl acid used to fix the pH of the IFF. As time goes by, the main peak changes in amplitude, frequency and phase, according to the concomitant redistribution of the magnetic particles of the ferrofluid, while forming the chain-like structures and superstructures. The spectra of Fig. 2c and d are the representative of the state reached at 3000 s, where mainly bundles of hexagonal zipped-chain patches are present in the fluid.[16] It is important to emphasize that this final steady-state reached at the end of every long NMR measurement run is an equilibrium state, provided the magnetic field remains applied. On the contrary, in the absence of any magnetic field (the sample is taken out of the NMR spectrometer, for example) the state characterized by chain-like structures and superstructures is metastable. In fact, after a day or so under ambient conditions or by immersing the sample in an ultrasound bath, the ferrofluid returns to its initial state of colloidally dispersed nanoparticles (monomers). This was experimentally verified by comparing the NMR spectra of the sample after sonication (before every measurement run) with the NMR spectrum of the original pristine sample.

Fig. 3 shows the evolution of the two main parameters, amplitude and frequency shift, of the dominant peak in the NMR spectra (real part) for different dwelling times in the external magnetic field gradient. Fig. 3a displays the time evolution up to 2500 s of the amplitude (black curve) and the frequency shift (red curve) for the case of the pristine sample (no external magnetic field gradient was applied), corresponding to the data published

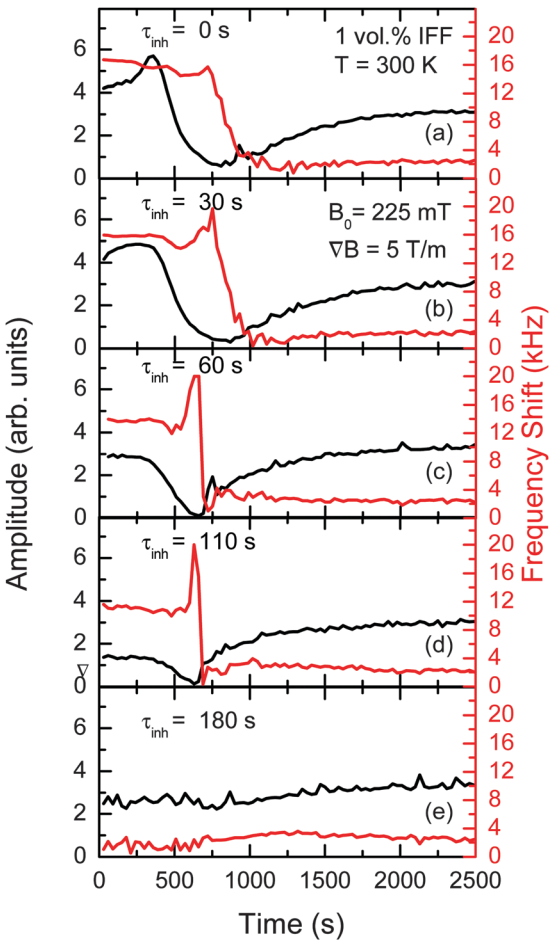

Fig. 3 Time evolution of the amplitude (black line) and the frequency shift (red curve) of the real part of the FID signal measured for the IFF sample after different dwelling times τ_{inh} of (a) 0 s, (b) 30 s, (c) 60 s, (d) 110 s, and (e) 180 s in an external magnetic field gradient of roughly 5 T m^{-1}.

elsewhere.[16] Fig. 3b–e display the NMR results obtained after the IFF sample was sitting for τ_{inh} = 30, 60, 110 and 180 s in the inhomogeneous field, respectively. We point out that in contrast to the clear changes observed for the dominant peak in NMR spectra, the weak and broad features corresponding to the pure water and HCl protons show only very small variations in all parameters with time.

The abrupt change in the frequency of the main peak allows for a distinction between two stages in the time evolution of the aggregation state of the IFF. In contrast, the linewidth and phase shift values (not shown) vary relatively little during the whole measurement run. The first stage corresponds to the period of gradual aggregation of monomers prior to and during the formation of chains.[16] As already mentioned, the frequency shift of about 17 kHz is indicative of a strong average magnetic field produced by the oriented magnetic moments of the grains. The second stage, characterized by a much smaller frequency shift of about 2 kHz, proceeds after the chains have reached a critical average length. Molecular dynamics (MD) simulations in a homogeneous field have shown that at this point the sluggish formation of patches of a locally crystalline superstructure, consisting of bundles of field-oriented, parallel staggered chains, sets in.[16] The small frequency shift is indicative of a much lower average magnetic field created by the chain bundles. We point out that the apparent peak in the frequency shift at measurement times around 600 to 800 s is due to spurious artifacts generated by the fitting procedure, for at those times the amplitude of the FID signal is at its absolute minimum and the error in the determination of the frequency is maximal.

Regarding the amplitude of the main peak, we observe that during the first stage it remains approximately constant (or increases slightly) for the first 400 s and then a steep decrease in intensity sets in. As discussed in ref. 16, this decrease signalizes the beginning of chain-segment formation and is explained by the fact that each time two particles form a dimer or one particle adds to a chain, there is a loss of two high field regions corresponding to the magnetic poles which are now in contact. Hence, chain formation leads to a continuous decrease in the number of protons in high field shift regions, the ones contributing to the main NMR peak (large frequency shift). Close after the point where the amplitude of the main peak ($\sim$17 kHz) reaches its minimum, the chain segments have reached the critical length for agglomeration into zipped-chain bundles. This is the starting point of the second stage which is characterized by a low-frequency peak ($\sim$2 kHz) that grows continuously in amplitude, indicating the steady formation of the chain bundles. Such lateral aggregation is further favored by an effective attractive vdW interaction.[16] From Fig. 3b–e we can anticipate that the main effect of magnetophoresis appears to be an acceleration of the aggregation process. Depending on how long the IFF dwelled in the field gradient, the ferrofluid is brought to a state of aggregation where longer chains or even superstructures have been formed. For example, for τ_{inh} = 180 s (see Fig. 3e) the formation of the zipped-chain bundles had already clearly started in the inhomogeneous field. Interestingly, whatever the aggregation state reached by magnetophoretic motion might be, from that point on the system appears to evolve exactly in the same manner as in the homogeneous field B_0 of the NMR spectrometer.

The results of MD simulations are in excellent qualitative agreement with this two-stage dynamics of nanograin aggregation in the presence of a homogeneous magnetic field.[16] The quasi-instantaneous correlation functions of the particles parallel and normal to the field-direction ($g_{\parallel}(r_{ij})$, $g_{\perp}(r_{ij})$), respectively, were also used to assist in the interpretation.[46] The simulations show that at the beginning of the dynamics, the typical configuration involves only monomers. As MD simulation time elapses, a regime involving association of particles into strings oriented along the field direction was observed. String formation was evidenced by the development of large peaks, separated by well-defined minima, in the quasi-instantaneous correlation function $g_{\parallel}(r_{ij})$ of the particles in the field-direction. Consistent with the presence of individual strings, the function $g_{\perp}(r_{ij})$ is essentially zero at earlier times in the dynamics. However, the situation changes at later times, where MD results reveal lateral association of the strings into bundles with hexagonal-like ordering of the particles, as indicated by the appearance of non-zero values for $g_{\perp}(r_{ij})$. Additionally, the main peak of $g_{\perp}(r_{ij})$ is shifted towards somewhat larger distances relative to that of $g_{\parallel}(r_{ij})$, consistent with the fact that the particles in two neighboring chains tend to be shifted by half a particle diameter relative to one another (zipped-chain configuration).[16] This arrangement is known to minimize the energy in systems of aligned dipolar chains[6,28,47] and has also been observed in MC simulations of strongly coupled, confined dipolar systems.[48] In addition, there is experimental evidence for this kind of ordering from small-angle neutron scattering,[7] cryogenic electron transmission microscopy[8] and light scattering and transmission.[12] Finally, at long times in the magnetic field, MD simulations show that the system equilibrates at a state dominated by the presence of large chain bundles, exhibiting pronounced longitudinal and lateral correlations extending over several particle diameters.

In Fig. 4 we plot the mean chain length as a function of time, obtained by MD simulations (homogeneous field). To compute this quantity, two particles were considered aggregated if their separation was $r_{ij} \leq r_c = 1.5\sigma$. The MD results shown in Fig. 3 of ref. 16 clearly indicate that zipped-chain bundle formation starts roughly around a simulation time $t \approx 5 \times 10^4 \Delta t$, when the lateral correlation function $g_{\perp}$ begins to develop the first peak. At this time, the average chain length is $\langle N \rangle \approx 4$ (see Fig. 4). Later on, although bundles are being formed, chains continue to grow in length at a faster pace up to a time $t \approx 3 \times 10^5 \Delta t$, where the longitudinal correlation function $g_{\parallel}$ saturates.[16] As a consequence, the average chain length shown in Fig. 4 also stabilizes at a value of $\langle N \rangle \approx 25$. That means that at this second stage, chains do no grow any further in length and aggregation into zipped-chain bundles runs at full speed. We associate this point with the occurrence of the minimum in the amplitude of the 17 kHz peak in coincidence with the appearance of the 2 kHz peak in the NMR spectra of the IFF, as observed in Fig. 3. It is instructive to compare these results with the predictions of the model of chain formation introduced in Section 2.3. Using the sample parameters

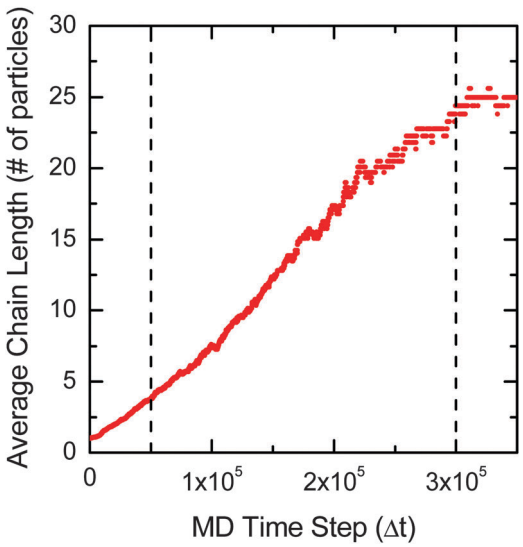

Fig. 4 Molecular dynamics results corresponding to the time evolution of the average chain length of IFF particles in the presence of a homogeneous magnetic field.

and eqn (7), we obtain for the magnetic coupling constant a value of $\Gamma = 11.9$. For our experimental volume fraction of $\phi_0 = 0.01$, mean-field theory [eqn (8)] predicts an average chain length of $\langle N \rangle = 23.6$. This value is in remarkable agreement with the results of MD simulations, though the latter were performed for a slightly larger volume fraction of $\phi_0 = 0.015$. Besides, the value of $\langle N \rangle$ is much larger than the minimum chain length of 14 monomers, which is necessary for lateral aggregation to become more favorable due to the minimization of the magnetic energy (in addition, bundles are more rigid and thermally stable).[29]

We now turn to a detailed analysis of the time variation of the main peak amplitude during the first evolution stage, for it provides deeper insight into the aggregation process in a homogeneous field and on the influence of magnetophoresis upon it. As mentioned before, it is evident from the time evolution of the amplitude parameter A (see Fig. 3a–e) that, irrespective of the time the IFF dwelled in the inhomogeneous field, the system always needs about 400 s before the marked decay in amplitude becomes detectable. This is clear evidence for complex structure-formation processes which cannot be described by a time-independent (constant) aggregation probability. If this were the case, $A(t)$ would exhibit a simple exponential decay with a characteristic time constant τ_{agg}. Let us first consider the underlying physical processes that might lead to the observed unusual behavior. In the absence of any magnetic field (outside the NMR spectrometer), the magnetic nanoparticles are uniformly distributed and there is no measurable magnetization. Notice that this is also true even in the case the colloid was subjected to an external gradient and chains of certain average length (depending on τ_{inh}) are dominantly present instead of monomers. We have previously measured by Raman scattering the characteristic time needed by the same IFF sample to recover a homogeneous density distribution, if the inhomogeneous magnetic field disturbing the particle density suddenly disappears.[9] This time is at room temperature roughly 45 s, whereas the typical time that elapses when the vial is transferred from the permanent magnet producing the gradient into the NMR spectrometer is about 1 min. Once inside the spectrometer, its highly homogeneous magnetic field polarizes the superparamagnetic fluid, leading to a massive alignment of the dipoles of monomers or chain pieces along B_0. Then, an attractive dipole–dipole interaction between the colloid constituents sets in. At the beginning, this interaction is weak but as time goes on, the head-to-tail attraction increasingly induces segregation of the colloid into a sort of three-dimensional network with regions of filamentary form with higher particle density. This can be "visualized" in the ESI† (Videos),[49] where we show the aggregation dynamics in the initial evolution stage. The denser the filaments, the faster the chain formation becomes. This is the point when the main NMR peak starts to exhibit its decay in amplitude, for the reasons stated before.

In order to describe quantitatively the time dependence of the amplitude A in Fig. 3, we take into account recent theoretical developments in the theory of relaxation in complex systems,[50,51] where the relaxation of the logarithm of the density follows a power law of the form t^{β}. The case $\beta < 1$ corresponds to the classical stretched exponential relaxation behavior observed in glasses. In recent times, the case $\beta > 1$ (compressed exponential behavior) has received considerable attention, since it has been found to hold in simulations and NMR experiments of gels and other soft glassy materials.[52,53] The underlying physics of a stretched or compressed exponential behavior is very different. Stretched exponentials correspond to a combination of different exponential relaxations with multiple time scales. In contrast, compressed exponentials imply a suppression of any fast relaxation channel. It has been suggested that a compressed exponential represents a non-diffusive but slow dynamics dominated by local drift of structures related to cooperative effects and dynamical heterogeneities. Previous work[44] has shown that at the concentrations considered here, the motion of magnetic particles in inhomogeneous fields leads to cooperative magnetophoresis. Therefore, our ansatz is that the aggregation probability is a monotonically growing function of time given by a simple power law with an exponent larger than one. The differential equation describing the evolution of the amplitude parameter, *i.e.*, the amount of aggregation, at the initial stage can thus be written as

$$\frac{\mathrm{d}A}{A} = -\frac{t^{n-1}}{\tau_{agg}^{n}} \cdot \mathrm{d}t. \tag{10}$$

Direct integration leads to the solution

$$A(t) = A_0 \cdot \exp\left[-\frac{1}{n} \cdot \left(\frac{t}{\tau_{agg}}\right)^{n}\right]. \tag{11}$$

In Fig. 5, we have plotted again the values of the main peak amplitude (symbols) as a function of time but solely in the first evolution stage up to about 900 s for different times τ_{inh} in the field gradient. The solid red curves represent the results of fits to

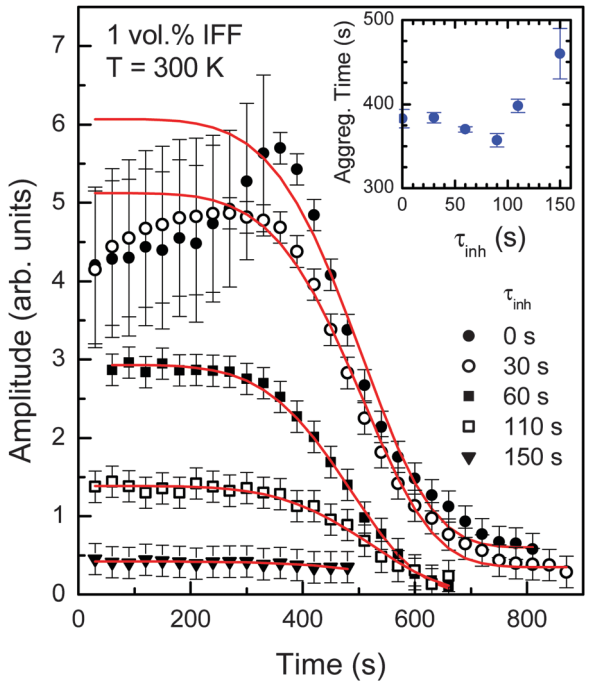

Fig. 5 Dependence on time of the amplitude (symbols) of the real part of the FID signal within the first stage of its evolution for different dwelling times τ_{inh} in the magnetic field gradient. Red curves correspond to a fit through the amplitude data points using eqn (11). The inset shows the values of the characteristic aggregation time τ_{agg} in a homogeneous field obtained from the fit as a function of the time τ_{inh} the IFF dwelled in the field gradient.

the data points using eqn (11), having only A_0 and τ_{agg} as adjustable parameters.

The exponent n was kept constant at a value of $n = 5$, which yielded the best fits (note that the simple exponential decay is recovered for $n = 1$). The compressed-exponential function of eqn (11) seems to capture the essential physics of the aggregation process in a homogeneous magnetic field for all the different initial aggregation states produced by exposing the IFF to a field gradient during different lapses. We note again that such a behavior has been observed in other soft materials, but with somewhat smaller exponents. On the contrary, eqn (11) cannot account for the slight increase in signal amplitude at short times observed for the curves corresponding to $\tau_{inh} = 0$ and 30 s; a behavior which remains elusive. The inset to Fig. 5 shows the values of the characteristic aggregation time τ_{agg} obtained from the fits. For times in the inhomogeneous field shorter than 150 s, the aggregation time is fairly constant and of the order of 400 s. For larger values of τ_{inh}, at which long chains or even zipped-chain bundles are majority, τ_{agg} tends to be a bit longer ($\approx$450 s), probably due to the fact that the density of larger aggregates is lower. In fact, a fit using a single exponential growth function yields a time constant for stage 2 of 420 $\pm$ 50 s.[16]

Regarding the influence of an inhomogeneous magnetic field, the representative results of Fig. 3 provide evidence that magnetophoresis does not seem to significantly alter the two-stage time evolution of the IFF. In order to perform a quantitative analysis, we have plotted in Fig. 6 as a function of the dwelling time τ_{inh} in the field gradient both the frequency shift and the amplitude of the main peak in the NMR spectrum at $\approx$30 s (black symbols) and at $\approx$3000 s (red symbols) of each measurement series. These correspond to the starting and ending conditions, respectively, in each run. From the measured frequency shifts at the beginning of the series, we infer that the IFF remains in stage 1, characterized by the coexistence of monomers and chain segments, up to a dwelling time of τ_{inh} = 150 s. The longer the dwelling time, the smaller the initial amplitude, which is simply due to the prolonged magnetophoretic action of the external gradient, promoting chain-segment formation. The frequency shift also exhibits a relatively small decrease, which might be an indication that the average magnetic field produced by the composite colloidal suspension of chains and monomers also decreases, if the number of the latter diminishes. For times $\tau_{inh} > 150$ s the IFF encounters itself already in stage 2, consisting principally of a suspension of zipped-chain bundles that just grow in size at the expense of the remaining chains. The final state reached by the IFF sample after the amplitude of the low-frequency peak (2 kHz) saturates, in contrast, is always the same, indicating that in the presence of a homogeneous magnetic field (that of the NMR

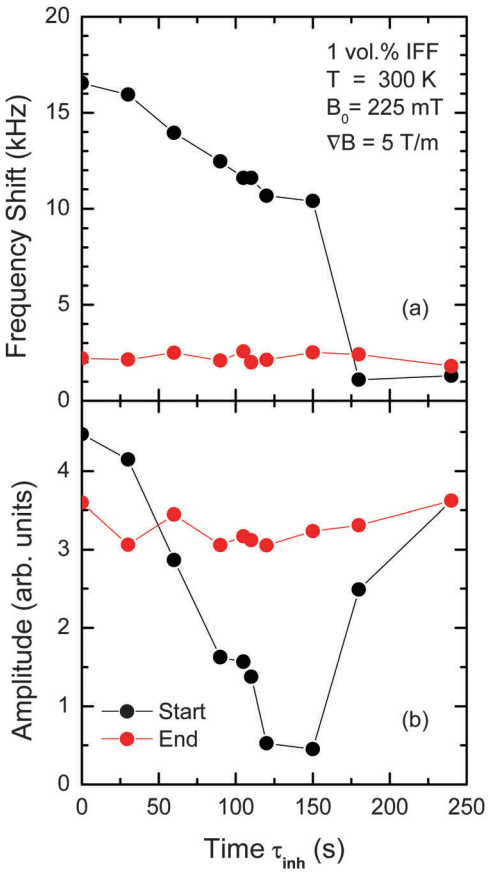

Fig. 6 (a) Frequency shift and (b) amplitude of the main NMR peak of the ionic ferrofluid at the beginning ($\approx$30 s, black symbols) and the end ($\approx$3000 s, red symbols) of each measurement series as a function of the exposure time to the external magnetic field gradient.

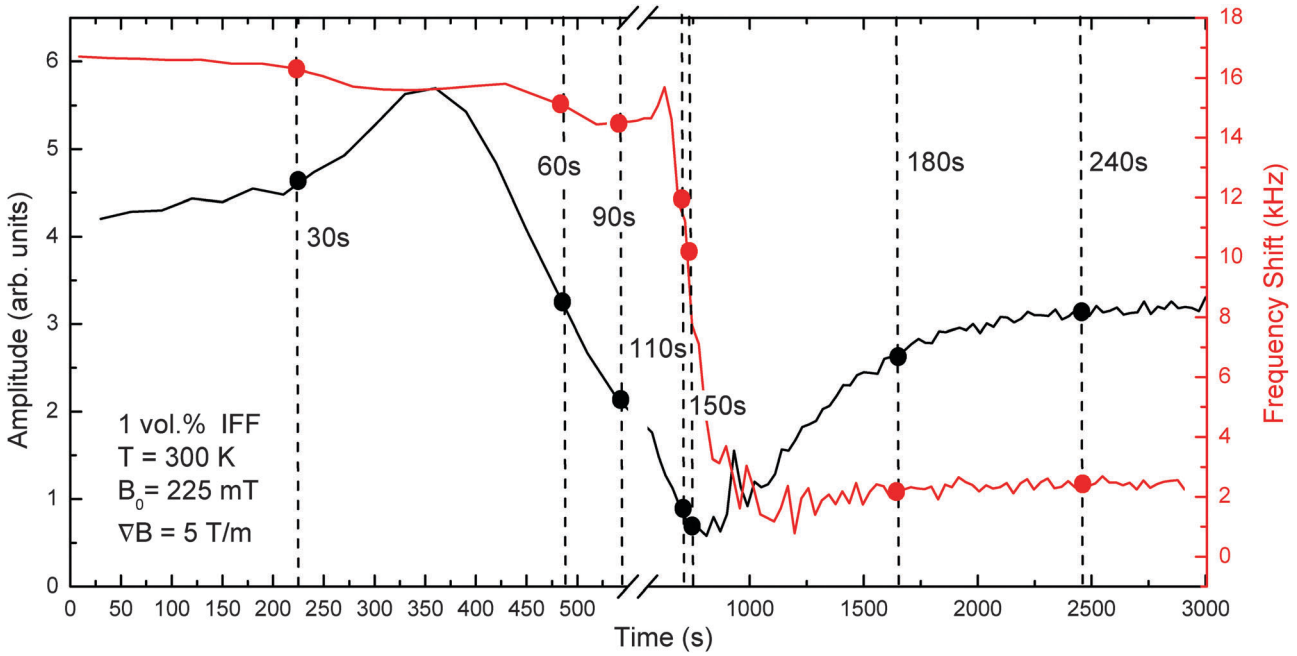

Fig. 7 Time evolution of the amplitude (black curve) and the frequency shift (red curve) of the main NMR peak measured for the pristine IFF sample (τ_{inh} = 0) every 30 s for times up to 3000 s. The black and red closed circles correspond to the amplitude and frequency at the beginning of a similar measurement series but performed after the IFF was sitting for a time τ_{inh} in the external magnetic field gradient, as indicated.

spectrometer, in this case) the equilibrium phase of an ionic ferrofluid with strong dipolar magnetic interactions consists of a suspension of zipped-chain bundles.

The main result of this work is illustrated in synthetic form with the help of the graph shown in Fig. 7. There, we depict again the time evolution up to 3000 s of the amplitude and the frequency shift of the main NMR peak measured for the pristine IFF sample. The key point is that we can mark on top of both curves the initial amplitude and frequency values (black and red closed circles), as obtained from the data points of Fig. 6, corresponding to the parameters determined at the beginning of a measurement series performed after the IFF was sitting for different times τ_{inh} in the external magnetic field gradient. For each τ_{inh} we can associate a time in the evolution of the pristine IFF sample, denoted by the dashed vertical lines, for which the aggregation state of the IFF in a homogeneous magnetic field would be the same as the one reached after dwelling τ_{inh} in the external magnetic field gradient. This holds true as far as the NMR signal is concerned. At this point, it is interesting to compare our results on the aggregation dynamics of magnetic nanoparticles with those obtained from magnetophoretic separation data,[44] since analysis of scaling laws in the latter case leads to a similar conclusion. In magnetophoresis separation experiments, a suspension of magnetic particles is placed in an inhomogeneous magnetic field with a gradient pointing towards the walls of the container. After a certain time (the separation time t_{sep}), the particles accumulate on the walls. The experimentally observed dependence of t_{sep} on the initial concentration of particles ($t_{sep} \sim \phi_0^{-1/4}$) can be justified theoretically only by a balance of hydrodynamic and magnetic forces, assuming that the aggregation kinetics follows the same functional form in homogeneous as well as inhomogeneous magnetic fields.

5 Concluding remarks

Our experimental as well as theoretical results indicate that the time evolution of the aggregation state of the IFF system proceeds in two stages, when subjected to a homogeneous magnetic field of a few hundreds of mT for long periods of time in the range of an hour. The first stage corresponds to a period of gradual aggregation of monomers prior to and during the formation of chains. The second stage proceeds after the chains have reached a critical average length and lateral association of the strings into the zipped-chain bundles takes place. The equilibrium state of the IFF system in an external magnetic field is precisely the one where the bundle-like superstructures are predominantly present, characterized by pronounced longitudinal and lateral correlations extending over several particle diameters. In the homogeneous field B_0 = 225 mT of the NMR spectrometer, all aggregation processes during both stages appear to take a time of the order of 400 s. Magnetophoresis is found to produce solely an acceleration of the aggregation dynamics, bringing the colloidal suspension (in a time scale of seconds) to a certain aggregation state which finds its correspondence to a state on the evolution curve of the pristine sample in a homogeneous field. Within the time interval that takes to withdraw the IFF from the external magnetic field gradient and to insert it into the bore of the NMR spectrometer, diffusive as well as convective motion of the magnetic entities of the colloidal suspension erases any concentration gradient which magnetophoresis might have established

during the time τ_{inh}. The degree of aggregation reached at the time τ_{inh}, though, is retained and the IFF sample just evolves thereafter in the homogeneous field of the spectrometer on a longer time scale of minutes in exactly the same way as the pristine sample. The final equilibrium state in the presence of a homogeneous magnetic field is that of a colloidal suspension of zipped-chain bundles with the chain axes aligned along the magnetic field direction, at least, at room temperature.

In this way, we have provided deeper insight into the processes governing aggregation dynamics in colloidal suspensions of magnetic nanoparticles and the role played by magnetophoretic effects. The latter are of particular importance for applications where the magnetic particles are driven and/or guided within the fluid by field gradients, mainly in view of the fact that larger aggregates are known to move much faster than smaller ones, due to the phenomenon of cooperative magnetophoresis.[29]

Acknowledgements

Special thanks are due to N. Buske from MagneticFluids for the ferrofluid samples. This work was supported by DAAD, Germany, and SECYT, Argentina, through the PROALAR2007 program. S. H. L. K. was supported by the German DFG within the priority program SPP 1681. T. M. O., L. M. C. C. and D. J. P. thank CONICET, Argentina, for financial support.

References

1 S. Odenbach, *Ferrofluids*, Springer, 2002, vol. 594.
2 C. P. Bean and J. D. Livingston, *J. Appl. Phys.*, 1959, **30**, S120.
3 A.-H. Lu, E. L. Salabas and F. Schüth, *Angew. Chem., Int. Ed.*, 2007, **46**, 1222.
4 M. Knobel, W. C. Nunes, L. M. Socolovsky, E. De Biasi, J. M. Vargas and J. C. Denardin, *J. Nanosci. Nanotechnol.*, 2008, **8**, 2836.
5 *Magnetic Nanoparticles*, ed. S. P. Gubin, Wiley-VCH, 2009.
6 E. M. Furst and A. P. Gast, *Phys. Rev. E: Stat. Phys., Plasmas, Fluids, Relat. Interdiscip. Top.*, 2000, **62**, 6916.
7 A. Wiedenmann, A. Hoell, M. Kammel and P. Boesecke, *Phys. Rev. E: Stat., Nonlinear, Soft Matter Phys.*, 2003, **68**, 031203.
8 M. Klokkenburg, B. H. Erne, J. D. Meeldijk, A. Wiedenmann, A. V. Petukhov, R. P. A. Dullens and A. P. Philipse, *Phys. Rev. Lett.*, 2006, **97**, 185702.
9 D. Heinrich, A. R. Goñi and C. Thomsen, *J. Chem. Phys.*, 2007, **126**, 124701.
10 W.-X. Fang, Z.-H. He, X.-Q. Xu, Z.-Q. Mao and H. Shen, *Europhys. Lett.*, 2007, **77**, 68004.
11 F. Martinez-Pedrero, *et al.*, *Phys. Rev. E: Stat., Nonlinear, Soft Matter Phys.*, 2008, **78**, 011403.
12 J. M. Laskar, J. Philip and B. Raj, *Phys. Rev. E: Stat., Nonlinear, Soft Matter Phys.*, 2009, **80**, 041401.
13 A. Wiedenmann, U. Keiderling, K. Habicht, M. Russina and R. Gähler, *Phys. Rev. Lett.*, 2006, **97**, 057202.
14 C. Rablau, P. Vaishnava, C. Sudakar, R. Tackett, G. Lawes and R. Naik, *Phys. Rev. E: Stat., Nonlinear, Soft Matter Phys.*, 2008, **78**, 051502.
15 F. Donado, U. Sandoval and J. L. Carrillo, *Phys. Rev. E: Stat., Nonlinear, Soft Matter Phys.*, 2009, **79**, 011406.
16 D. Heinrich, A. R. Goñi, A. Smessaert, S. H. L. Klapp, L. M. C. Cerioni, T. M. Osán, D. J. Pusiol and C. Thomsen, *Phys. Rev. Lett.*, 2011, **106**, 208301.
17 S. H. Lee and C. M. Lindell, *Small*, 2009, **5**, 1957.
18 C.-H. Chang, C.-W. Tan, J. Miao and G. Barbatathis, *Nanotechnology*, 2009, **20**, 495301.
19 T. Tlusty and A. A. Safran, *Science*, 2000, **290**, 1328.
20 J. Stambaugh, K. van Workum, J. F. Douglas and W. Losert, *Phys. Rev. E: Stat., Nonlinear, Soft Matter Phys.*, 2005, **72**, 031301.
21 P. D. Duncan and P. J. Camp, *Phys. Rev. Lett.*, 2006, **97**, 107202.
22 A. Goyal, C. K. Hall and O. D. Velev, *Soft Matter*, 2010, **6**, 480.
23 J. J. Weis, *Mol. Phys.*, 2005, **103**, 7.
24 A.-P. Hynninen and M. Dijkstra, *Phys. Rev. Lett.*, 2005, **94**, 138303.
25 J. E. Martin, R. A. Anderson and C. P. Tigges, *J. Chem. Phys.*, 1998, **108**, 3765.
26 P. Ilg, *Eur. Phys. J. E: Soft Matter Biol. Phys.*, 2008, **26**, 169.
27 T. C. Halsey and W. Toor, *Phys. Rev. Lett.*, 1990, **65**, 2820.
28 R. Tao and J. M. Sun, *Phys. Rev. Lett.*, 1991, **67**, 398.
29 J. Faraudo and J. Camacho, *Colloid Polym. Sci.*, 2010, **288**, 207–215.
30 S. Gangwal, A. Pawar, I. Kretzschmar and O. D. Velev, *Soft Matter*, 2010, **6**, 1413.
31 C. W. Shields IV, S. Zhu, Y. Yang, B. Bharti, J. Liu, B. B. Yellen, O. D. Velev and G. P. López, *Soft Matter*, 2013, **9**, 9219.
32 E. Taboada, R. Solanas, E. Rodrguez, R. Weissleder and A. Roig, *Adv. Funct. Mater.*, 2009, **19**, 2319–2324.
33 J. L. Corchero and A. Villaverde, *Trends Biotechnol.*, 2009, **27**, 468.
34 I. Safarik and M. Safarikova, *BioMagn. Res. Technol.*, 2004, **2**, 7.
35 *Colloidal Magnetic Fluids Basics, Development and Application of Ferrofluids*, ed. S. Odenbach, Springer, 2009, vol. 763.
36 J. E. Weber, A. R. Goñi, D. J. Pusiol and C. Thomsen, *Phys. Rev. E: Stat., Nonlinear, Soft Matter Phys.*, 2002, **66**, 021407.
37 J. E. Weber, A. R. Goñi and C. Thomsen, *J. Magn. Magn. Mater.*, 2004, **277**, 96.
38 C. E. González, D. J. Pusiol, A. M. Figueiredo Neto, M. Ramia and A. Bee, *J. Chem. Phys.*, 1998, **109**, 4670.
39 M. H. Levitt, *Spin Dynamics: Basics of Nuclear Magnetic Resonance*, Wiley, 2nd edn, 2008.
40 E. Fukushima and B. W. Roeder, *Experimental Pulse NMR: A Nuts and Bolts Approach*, Addison-Wesley, Massachusetts, 1981.
41 The screened dipole–dipole potential was originally constructed for dipolar molecules in electrolyte solutions.
42 M. P. Allen and D. J. Tildesley, *Computer Simulation of Liquids*, Academic, London, 1987.

43 J. S. Andreu, J. Camacho, J. Faraudo, M. Benelmekki, C. Rebollo and L. M. Martnez, *Phys. Rev. E: Stat., Nonlinear, Soft Matter Phys.*, 2011, **84**, 021402.
44 J. Faraudo, J. S. Andreu and J. Camacho, *Soft Matter*, 2013, **9**, 6654.
45 J. S. Andreu, J. Camacho and J. Faraudo, *Soft Matter*, 2011, **7**, 2336.
46 S. H. L. Klapp and M. Schoen, *J. Chem. Phys.*, 2002, **117**, 8050.
47 C. E. Alvarez and S. H. L. Klapp, *Soft Matter*, 2012, **8**, 7480.
48 R. A. Trasca and S. H. L. Klapp, *J. Chem. Phys.*, 2008, **129**, 084702.
49 See ESI† for further sample characterization and/or videos showing the aggregation dynamics in a short and long time scale, as obtained from the MD simulations.
50 J.-P. Bouchaud, Cond-mat arXiv: 0705.0989, 2007, http://arxiv.org/abs/0705.0989.
51 J.-P. Bouchaud, Anomalous transport: foundations and applications, in *Anomalous Relaxation in complex systems: from stretched to compressed exponentials*, ed. R. Klages, G. Radons and I. M. Sokolov, Wiley, 1st edn, 2008, ch. 11.
52 E. W. Hansen, X. Gong and Q. Chen, *Macromol. Chem. Phys.*, 2013, **214**, 844.
53 S. Saw, N. L. Ellegaard, W. Kob and S. Sastry, *Phys. Rev. Lett.*, 2009, **103**, 248305.

